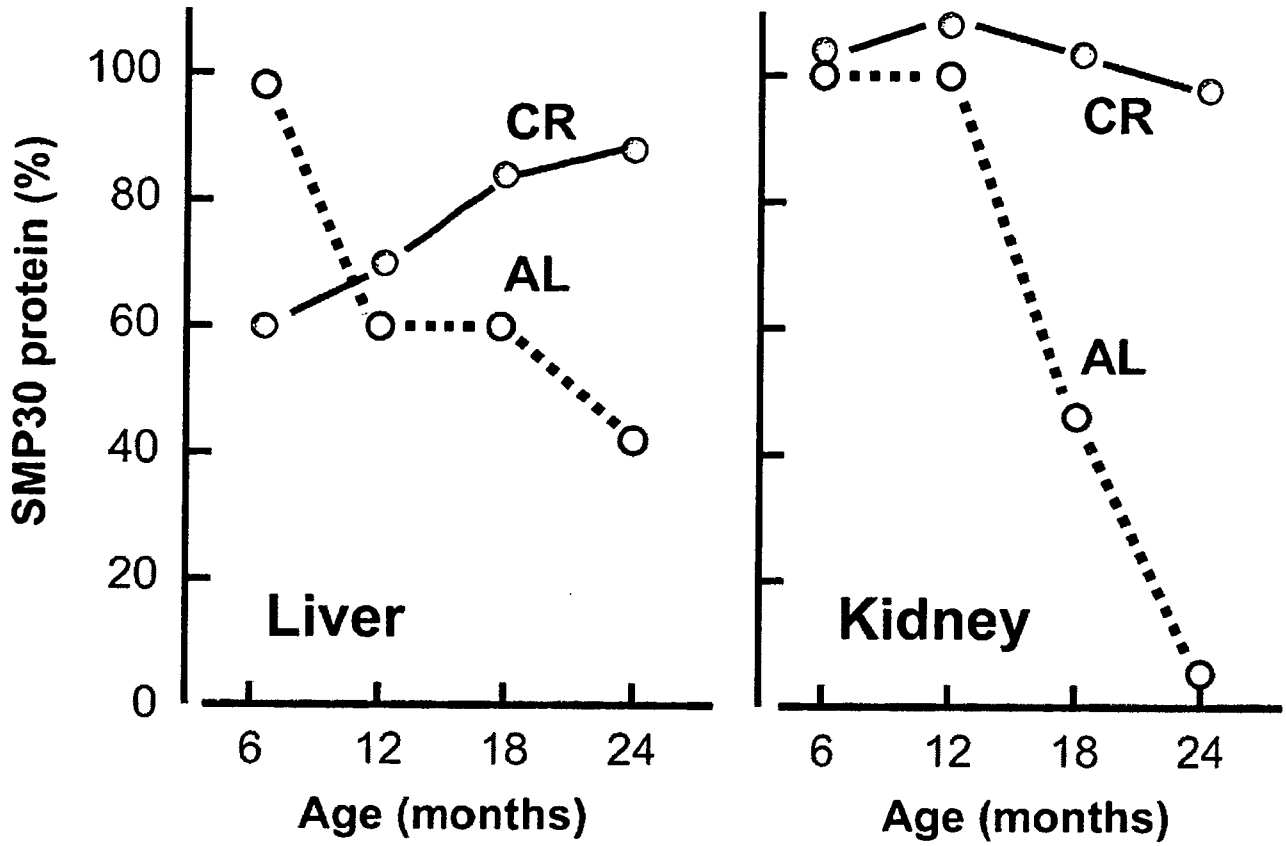

Figure 7 Enhanced SMP30 protein levels in the liver and kidneys from a calorie restricted (CR) diet. Rats were divided into an ad libitum fed group (AD) and a 40% CR group.

this transcription factor to the two sites in the SMP30 promoter region decreased after treatment with t-BHP or LPS. These findings were confirmed by using the anti-oxidant NAC and the ERK-specific inhibitor PD098059, both of which blunted the decrease in *SMP30* gene expression. Third, the binding by t-BHP also diminished at both sites in the Ac2F cell system. These outcomes strongly indicate that the SMP30 transcriptional process is redox-sensitive and that its modulation occurs at DNA binding sites in the promoter region. The downregulation of SMP30 likely involves the ERK signal pathway.

Conclusions

Proteomics analysis has provided us with a large amount of information about aging in general and, in particular, about age-associated molecules including SMP30. This factor is one of the best prospects for elucidating the mechanism of senescence, as we have done in functional analyses of multiple organs. We propose that the SMP30-knockout murine strain, in which SMP30 is completely absent, is the most useful model available for understanding human aging. In fact, the absence of SMP30 is the reason why this strain lacks an enzyme responsible for the synthesis of vitamin C as an anti-oxidant. Further research on the biological functions of SMP30 will assuredly produce useful tools for treating or offsetting the deleterious effects of aging in humans.

Acknowledgments

This work is supported by the NOVARTIS Foundation for Gerontological Research. A grant from the Japanese Ministry of Education, Culture, Sports, Science, and Technology and a grant from Health Science Research Grants for Comprehensive Research on Aging and Health supported by the Ministry of Health, Labor, and Welfare of Japan are acknowledged. The excellent assistance in the review of English by Ms P. Minick is gratefully acknowledged.

References

1 Tahara S, Kaneko T. Susceptibility of mouse splenic cells to oxidative DNA damage by x-ray irradiation. *Biol Pharm Bull* 2004; 27: 105–108.

2 Nawata H, Yanase T, Goto K, Okabe T, Ashida K. Mechanism of action of anti-aging DHEA-S and the replacement of DHEA-S. *Mech Ageing Dev* 2002; **123**: 1101–1106.
3 Hosokawa M. A higher oxidative status accelerates senescence and aggravates age-dependent disorders in SAMP strains of mice. *Mech Ageing Dev* 2002; **123**: 1553–1561.
4 Kuro-oM, Matsumura Y, Aizawa H *et al.* Mutation of the mouse klotho gene leads to a syndrome resembling ageing. *Nature* 1997; **390**: 45–51.
5 Fujita T, Uchida K, Maruyama N. Purification of senescence marker protein-30 (SMP30) and its androgen-independent decrease with age in the rat liver. *Biochim Biophys Acta* 1992; **1116**: 122–128.
6 Ishigami A, Handa S, Maruyama N, Supakar PC. Nuclear localization of senescence marker protein-30, SMP30, in cultured mouse hepatocytes and its similarity to RNA polymerase. *Biosci Biotechnol Biochem* 2003; **67**: 158–160.
7 Fujita T, Shirasawa T, Uchida K, Maruyama N. Isolation of cDNA clone encoding rat senescence marker protein-30 (SMP30) and its tissue distribution. *Biochim Biophys Acta* 1992; **1132**: 297–305.
8 Fujita T, Mandel JL, Shirasawa T, Hino O, Shirai T, Maruyama N. Isolation of cDNA clone encoding human homologue of senescence marker protein-30 (SMP30) and its location on the X chromosome. *Biochim Biophys Acta* 1995; **1263**: 249–252.
9 Fujita T, Shirasawa T, Maruyama N. Isolation and characterization of genomic and cDNA clones encoding mouse senescence marker protein-30 (SMP30). *Biochim Biophys Acta* 1996; **1308**: 49–57.
10 Goto SG. Expression of Drosophila homologue of senescence marker protein-30 during cold acclimation. *J Insect Physiol* 2000; **46**: 1111–1120.
11 Nakajima Y, Natori S. Identification and characterization of an anterior fat body protein in an insect. *J Biochem (Tokyo)* 2000; **127**: 901–908.
12 Kondo Y, Ishigami A, Kubo S *et al.* Senescence marker protein-30 is a unique enzyme that hydrolyzes diisopropyl phosphorofluoridate in the liver. *FEBS Lett* 2004; **570**: 57–62.
13 Fujita T, Inoue H, Kitamura T, Sato N, Shimosawa T, Maruyama N. Senescence marker protein-30 (SMP30) rescues cell death by enhancing plasma membrane Ca^{2+}-pumping activity in Hep G2 cells. *Biochem Biophys Res Commun* 1998; **250**: 374–380.
14 Inoue H, Fujita T, Kitamura T *et al.* Senescence marker protein-30 (SMP30) enhances the calcium efflux from renal tubular epithelial cells. *Clin Exp Nephr* 1999; **3**: 261–267.
15 Billecke SS, Primo-Parmo SL, Dunlop CS, Doorn JA, La Du BN, Broomfield CA. Characterization of a soluble mouse liver enzyme capable of hydrolyzing diisopropyl phosphorofluoridate. *Chem Biol Interact* 1999; **119–120**: 251–256.
16 Little JS, Broomfield CA, Fox-Talbot MK, Boucher LJ, MacIver B, Lenz DE. Partial characterization of an enzyme that hydrolyzes sarin, soman, tabun, and diisopropyl phosphorofluoridate (DFP). *Biochem Pharmacol* 1989; **38**: 23–29.
17 Gomi K, Kajiyama N. Oxyluciferin, a luminescence product of firefly luciferase, is enzymatically regenerated into luciferin. *J Biol Chem* 2001; **276**: 36508–36513.
18 Gomi K, Hirokawa K, Kajiyama N. Molecular cloning and expression of the cDNAs encoding luciferin-regenerating enzyme from Luciola cruciata and Luciola lateralis. *Gene* 2002; **294**: 157–166.
19 Kanagasundaram V, Scopes R. Isolation and characterization of the gene encoding gluconolactonase from Zymomonas mobilis. *Biochim Biophys Acta* 1992; **1171**: 198–200.
20 Kondo Y, Inai Y, Sato Y *et al.* Senescence marker protein 30 functions as gluconolactonase in l-ascorbic acid biosynthesis, and its knockout mice are prone to scurvy. *Proc Natl Acad Sci USA* 2006; **103**: 5723–5728.
21 Brodie AF, Lipmann F. Identification of a gluconolactonase. *J Biol Chem* 1955; **212**: 677–685.
22 Ishigami A, Fujita T, Inoue H *et al.* Senescence marker protein-30 (SMP30) induces formation of microvilli and bile canaliculi in Hep G2 cells. *Cell Tissue Res* 2005; **320**: 243–249.
23 Takeuchi K, Sato N, Kasahara H *et al.* Perturbation of cell adhesion and microvilli formation by antisense oligonucleotides to ERM family members. *J Cell Biol* 1994; **125**: 1371–1384.
24 Ando-Akatsuka Y, Yonemura S, Itoh M, Furuse M, Tsukita S. Differential behavior of E-cadherin and occludin in their colocalization with ZO-1 during the establishment of epithelial cell polarity. *J Cell Physiol* 1999; **179**: 115–125.
25 Ishigami A, Fujita T, Handa S *et al.* Senescence marker protein-30 knockout mouse liver is highly susceptible to tumor necrosis factor-α- and Fas-mediated apoptosis. *Am J Pathol* 2002; **161**: 1273–1281.
26 Matsuyama S, Kitamura T, Enomoto N *et al.* Senescence marker protein-30 regulates Akt activity and contributes to cell survival in Hep G2 cells. *Biochem Biophys Res Commun* 2004; **321**: 386–390.
27 Cheng A, Wang S, Yang D, Xiao R, Mattson MP. Calmodulin mediates brain-derived neurotrophic factor cell survival signaling upstream of Akt kinase in embryonic neocortical neurons. *J Biol Chem* 2003; **278**: 7591–7599.
28 Egea J, Espinet C, Soler RM *et al.* Neuronal survival induced by neurotrophins requires calmodulin. *J Cell Biol* 2001; **154**: 585–598.
29 Ishigami A, Kondo Y, Nanba R *et al.* SMP30 deficiency in mice causes an accumulation of neutral lipids and phospholipids in the liver and shortens the life span. *Biochem Biophys Res Commun* 2004; **315**: 575–580.
30 Mori T, Ishigami A, Seyama K *et al.* Senescence marker protein-30 knockout mouse as a novel murine model of senile lung. *Pathol Int* 2004; **54**: 167–173.
31 Sato T, Seyama K, Sato Y *et al.* Senescence marker protein-30 protects mice lungs from oxidative stress, aging, and smoking. *Am J Respir Crit Care Med* 2006; **174**: 530–537.
32 Ishii K, Tsubaki T, Fujita K, Ishigami A, Maruyama N, Akita M. Immunohistochemical localization of senescence marker protein-30 (SMP30) in the submandibular gland and ultrastructural changes of the granular duct cells in SMP30 knockout mice. *Histol Histopathol* 2005; **20**: 761–768.
33 Son TG, Zou Y, Jung KJ *et al.* SMP30 deficiency causes increased oxidative stress in brain. *Mech Ageing Dev* 2006; **127**: 451–457.
34 Clark RS, Carlos TM, Schiding JK. Antibodies against Mac-1 attenuate neutrophil accumulation after traumatic brain injury in rats. *J Neurotrauma* 1996; **13**: 333–341.
35 Yumura W, Imasawa T, Suganuma S *et al.* Accelerated tubular cell senescence in SMP30 knockout mice. *Histol Histopathol* 2006; **21**: 1151–1156.
36 Jung KJ, Ishigami A, Maruyama N *et al.* Modulation of gene expression of SMP-30 by LPS and calorie restriction during aging process. *Exp Gerontol* 2004; **39**: 1169–1177.

37 Lane MA, Baer DJ, Rumpler WV *et al.* Calorie restriction lowers body temperature in rhesus monkeys, consistent with a postulated anti-aging mechanism in rodents. *Proc Natl Acad Sci USA* 1996; **93**: 4159–4164.
38 Jung KJ, Maruyama N, Ishigami A, Yu BP, Chung HY. The redox-sensitive DNA binding sites responsible for age-related downregulation of SMP30 by ERK pathway and reversal by calorie restriction. *Antioxid Redox Signal* 2006; **8**: 671–680.
39 Supakar PC, Fujita T, Maruyama N. Identification of novel sequence-specific nuclear factors interacting with mouse senescence marker protein-30 gene promoter. *Biochem Biophys Res Commun* 2000; **272**: 436–440.

Acta Oto-Laryngologica, 2007; 127: 1024–1030

informa
healthcare

ORIGINAL ARTICLE

Quantitative analysis of mRNA in human temporal bones

YURIKA KIMURA[1,2,3], SACHIHO KUBO[2], HIROKO KODA[3], YOSHIHIRO NOGUCHI[3], MOTOJI SAWABE[4], NAOKI MARUYAMA[2] & KEN KITAMURA[3]

[1]*Departments of Otolaryngology and* [4]*Pathology, Tokyo Metropolitan Geriatric Hospital,* [2]*Aging Regulation Group, Research Team for Molecular Biomarkers, Tokyo Metropolitan Institute of Gerontolog and* [3]*Department of Otolaryngology, Graduate School, Tokyo Medical and Dental University, Tokyo, Japan*

Abstract

Conclusion. Well-preserved mRNA could be extracted from frozen human inner ears. Therefore, this study demonstrates that analysis of mRNA could be performed to study the molecular mechanisms of inner ear disorders using human specimens. *Objectives.* Analysis of RNA as well DNA is requisite to study the molecular mechanisms of inner ear disorders. Methods of isolating RNA from experimental animals have been established, while isolation of RNA from human inner ears is much more challenging. In the present study, we demonstrate a method by which messenger RNA (mRNA) was extracted from human inner ears and quantitatively analyzed. *Materials and methods. COCH* mRNA as well as *GAPDH* mRNA was extracted from membranous labyrinths dissected from three formalin-fixed and three frozen human temporal bones, removed at autopsy. The length of *COCH* mRNA and quantity of *GAPDH* mRNA was compared between the two groups by quantitative RT-PCR. *Results. COCH* mRNA could be amplified as much as 976 bp in all three frozen specimens. By contrast, it was amplified to 249 bp in two of the three formalin-fixed specimens, with no amplification observed in the remaining. The quantity of amplifiable *GAPDH* mRNA in the formalin specimens was only 1% of that of the frozen specimens.

Keywords: *Hearing loss, human, inner ear, mRNA, PCR*

Introduction

The mechanisms of sensorineural hearing loss have been analyzed with the recent advent of advanced molecular techniques. Studies of animals including mice have also contributed to identifying deafness genes and determining genotype–phenotype correlations [1,2]. In contrast, molecular analysis using human inner ear specimens is difficult because human inner ear specimens are inaccessible and formalin-fixed, celloidin-embedded temporal bone specimens are unsuitable for molecular analysis even though this method has been standard in histopathologic studies of the human temporal bones [3]. Nonetheless, there have been several reports in which DNA has been extracted from human inner ear specimens. Wackym et al. reported the first study using molecular biological techniques for human temporal bone pathology in 1993 [4]. They succeeded in amplifying mitochondria DNA by PCR and emphasized the difficulty of analyzing DNA from the human temporal bone because of the autolysis that occurs before fixation. They also reported PCR amplification of varicella-zoster virus DNA from temporal bone sections [5], as well as histopathologic analysis of a patient with Ramsay Hunt syndrome [6]. Moreover, the possibility of a relationship between presbycusis and a 4977 bp mtDNA deletion was suggested by PCR amplification of mtDNA from the cochlea of a celloidin-embedded human archival temporal bone [7]. We recently reported a quantitative analysis of mtDNA from a patient with a mutation at nucleotide 3243 [8] and detection of mitochondrial DNA from human inner ears using real-time PCR and laser microdissection [9] to elucidate mitochondrial hearing impairment. However, the availability of DNA analysis at a tissue level is limited to measurement of

Correspondence: Dr Ken Kitamura, Department of Otolaryngology, Tokyo Medical and Dental University, Graduate School, Yushima, Bunkyo-ku, Tokyo, 113-8519 Japan. Tel: +81 3 5803 5303. Fax: +81 3 5803 0146. E-mail: kitamura.oto@tmd.ac.jp

(Received 29 September 2006; accepted 14 December 2006)

ISSN 0001-6489 print/ISSN 1651-2551 online
DOI: 10.1080/00016480701200202

the heteroplasmy mutation ratio in mitochondrial hearing impairment or detection of a DNA virus, as mentioned above.

By contrast, analysis of mRNA expression patterns can demonstrate the spatio-temporal activities of gene transcription and expression in tissues, providing important physiological and pathological information at the molecular level [10]. Further, mRNA is important because it is a 'working copy' of a gene that directs biological activities of cells through the synthesis of proteins. Therefore, studying mRNA extracted from human inner ears can provide further information concerning the molecular mechanisms of inner ear disorders in humans. As removing temporal bones at autopsy is a regular method for studying human specimens, we analyzed and compared mRNA in formalin-fixed and frozen temporal bones removed at autopsy. The purpose of the present report was to establish the optimal method of extracting mRNA suitable for molecular biological applications from autopsied human temporal bones.

Materials and methods

Temporal bones

Six human temporal bones from five subjects with no hearing impairment (according to nursing records) were obtained at brain autopsy. Three were formalin-fixed and the others were put into the deep freezer as soon as possible after harvest and conserved by freezing at −80°C. The average age of the subjects was 77.0 years (range 72–83 years). The average time period between death and the start of autopsy was 20.1 h (range 4–47 h). Consent for using organs removed at autopsy was obtained from the patients' relatives. The present study was approved by the Ethical Review Board at Tokyo Metropolitan Geriatric Medical Hospital, pursuant to Article 18 of the Cadaver Autopsy and Preservation Act. Temporal bones were processed according to the surface preparation method (Figure 1) [11]. To avoid the degradation of RNA, we used RNAlater® (Ambion, Austin, TX, USA) to impregnate the temporal bone during the process and injected it into the inner ear from the oval window. The geniculate ganglion of facial nerves and the membranous labyrinth were dissected and immersed in a 1.5 ml microtube with 0.2 ml ISOGEN® (Nippon Gene, Tokyo, Japan).

Total RNA extraction and reverse transcription

Temporal bone samples were stored for an average of 7.5 months (range 2–18 months) before dissection. Dissected tissues were homogenized and mixed with 0.6 ml of ISOGEN®. After storage at room temperature for 5 min, 0.2 ml of chloroform was added. The mixture was shaken vigorously for 30 s, stored for 5 min at 4°C, and centrifuged at 15 000 g for 15 min at 4°C. The aqueous phase was transferred to microtubes, and 0.5 ml of chloroform was added. The mixture was shaken vigorously for 30 s, stored for 5 min at 4°C and centrifuged at 15 000 g for 15 min again. The supernatant was transferred and mixed with 0.5 μl of glycogen and 0.8 ml of isopropanol. After storage for >30 min at 4°C, the mixture was centrifuged at 15 000 g for 15 min at 4°C. The resultant supernatant was then carefully removed. The pellet containing RNA was washed with 70% ethanol three times, allowed to air-dry, and dissolved in 20 μl of RNase-free ddH_2O. The RNA concentration was determined by OD_{260}, measured by an ND-1000 Spectrophotometer® (NanoDrop, Wilmington, DE, USA). Approximately 40 ng of total RNA per sample was reverse transcripted in a 20 μl reaction using Transcriptor First Strand cDNA Synthesis Kit® (Roche, Basel, Switzerland) following the manufacturer's protocols.

PCR and sizing of PCR products

To compare the preserved length of mRNA between formalin-fixed and frozen samples, primers were designed using Primer 3 (http://frodo.wi.mit.edu/cgi-bin/primer3/primer3_www.cgi), on mRNA of *COCH* (accession no. NM004086), the coded protein of which is abundant in the inner ear [12]. Eight forward primers and one reverse primer were made to amplify 249–976 bp cDNA fragments (Figure 2). PCR was performed in a 20 μl volume containing 10 μl Premix Taq® (Takara Bio, Otsu, Japan), 0.5 μM of each specific primer and 1 μl of cDNA from the RT reaction. After initial incubation at 94°C for 3 min, the reaction mixtures were subjected to 35 cycles of amplification using the following sequence: 94°C for 30 s, 55°C for 30 s, and 72°C for 45 s. This was followed by a final extension step at 72°C for 7 min. Finally, 8 μl of the reaction mixture was run on a 2% agarose gel and visualized with ethidium bromide. Each amplification product was sequenced on an ABI PRISM® 3100 Genetic Analyzer (Applied Biosystems, Foster City, CA, USA).

Quantitative PCR analysis

To compare the quantity of mRNA for PCR level, quantitative real-time PCR was performed. TaqMan PCR® is a quantitative real-time PCR technique based on the 5′ exonuclease activity of TaqPolymerase [13]. In addition to the sense and antisense primers, a nonextendable oligonucleotide probe with

Figure 1. Temporal bones were processed according to the surface preparation method, and impregnated with RNAlater® (Ambion) to avoid the resolution of RNA. The membranous labyrinth was dissected. Arrows indicate pigmentation of stria vascularis.

a 5′ fluorescent reporter dye and a 3′ quencher dye were used. During the extension phase, Taq polymerase hydrolyzes the probe, thereby generating a fluorescent signal. In our experiment, this signal was monitored using 7300 Real-Time PCR System® (Applied Biosystems).

Primer name	Sequences	Product size
COCH-F1	TGATGACATCGAGGAAGCAG	249
COCH-F2	ACAGGAAAAGCCTTGAAGCA	356
COCH-F3	GCCAGTGAACATCCCAAAAT	461
COCH-F4	GCAGCGCCGATTTAATTTAC	555
COCH-F5	ACAAGCAGTGTCCACAGCAC	681
COCH-F6	GGCATCCAGTCTCAAATGCT	764
COCH-F7	TCCACAGGGGAGTAATCAGC	853
COCH-F8	GAGGCTTGGACATCAGGAAA	976
COCH-R	CAGGTCTTGCTGCACATCAT	

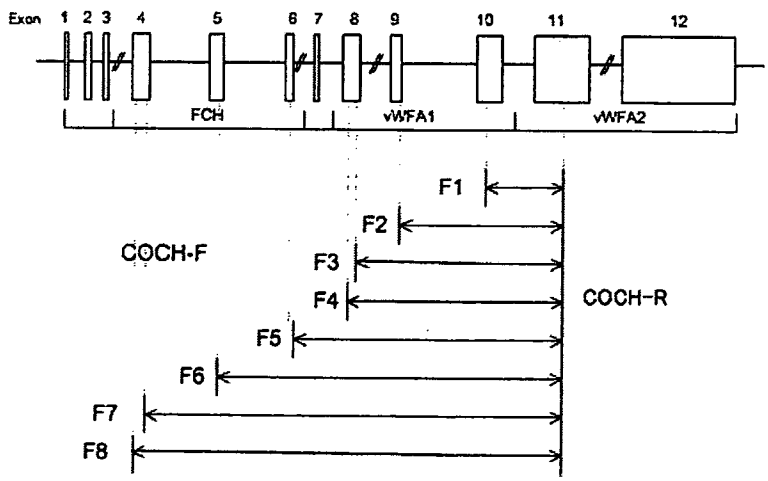

Figure 2. Primer sequences and amplified fragment size. Schematic drawing of the locus amplified by these primers in human *COCH* genomic structure. Exons are indicated by shaded boxes. The region of Limulus factor C homology (FCH) spans exon 4–6. The von Willebrand factor A-like domain, vWFA1, is contained in exon 8–10; vWA2 is in exon 11 and 12. Each primer set is in coding region.

We measured levels of *GAPDH*, which is a well-known housekeeping gene. PCR primers and probes were provided by TaqMan® GAPDH Control Reagents kit (ABI). PCR was performed in a 20 μl volume containing 10 μl Premix Ex Taq® (Takara Bio, Otsu, Japan), 0.2 μM of each specific primer, 0.1 μl of the GAPDH probe, 0.4 μl of Rox Reference Dye, and 1 μl of cDNA from the RT reaction. After initial incubation at 95°C for 10 s, the reaction mixtures were subjected to 45 cycles of amplification using the following sequence: 95°C for 5 s and 60°C for 31 s. This was followed by a final extension step: 95°C for 15 s, 60°C for 1 min and 95°C for 15 s. TaqMan PCR® was performed twice for each sample.

To quantify mRNA for PCR levels, we recorded the average number of PCR cycles (Ct) required for each reaction's fluorescence to cross a threshold value of intensity, set to pass through the linear portion of the amplification curve. Frozen samples were defined as standards, and the difference in Ct between the formalin-fixed samples and the standards was used to calculate dCt. The quantity relative to the standard was obtained from 2^{-dCt} [14]. The Student's t test was used for comparison between the two groups, and a probability value <0.05 was considered statistically significant.

Results

Total RNA yield

Average total RNA yield measured by ND-1000 Spectrophotometer® was 0.89 ± 0.40 μg of formalin-fixed samples and 2.73 ± 1.11 μg of frozen samples.

Comparison of the length of RT-PCR products for frozen and formalin-fixed samples

The results of the *COCH* mRNA RT-PCR amplification are shown in Figure 3a and b, in comparison to the RT-PCR product migration in the gel with the migration of a 50 bp ladder marker (lane 1). Lanes 2–9 show the results of the RT-PCR amplification using *COCH* primers. Amplification to 976 bp was possible in all three frozen samples. On the other hand, among the three formalin-fixed samples, two could be amplified to only 249 bp and the other could not be amplified with these primers. By sequencing the amplification product, these bands were confirmed as targeted locus.

Comparison of the quantity of real-time RT-PCR products between frozen and formalin-fixed specimens

The frozen samples were determined as standards, and the difference in Ct value between formalin-fixed samples and these standards was defined as

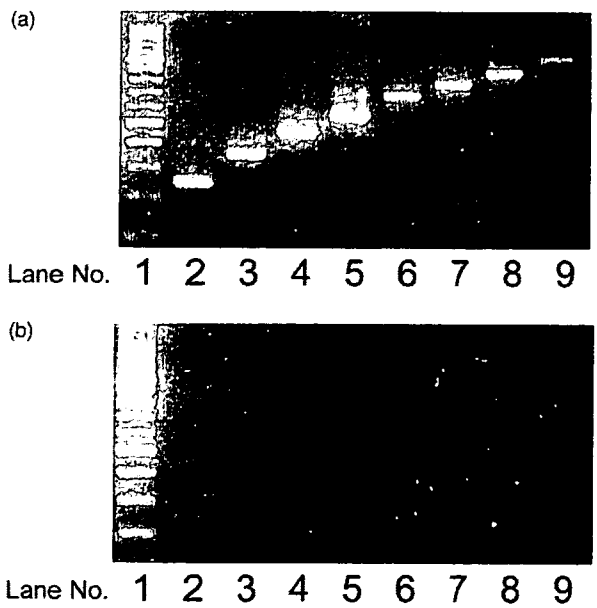

Figure 3. RT-PCR product migration in the gel with the migration of a 50 bp ladder marker (lane 1). Lanes 2–9 show the results of the RT-PCR amplification using *COCH* primers (a, frozen section; b, formalin-fixed sample). Amplification to 976 bp was possible in all three frozen samples; by contrast, two of the formalin-fixed samples could be amplified to only 249 bp and the other could not be amplified with these primers. Lane 2 shows a 249 bp fragment; lane 3, a 356 bp fragment; lane 4, 461 bp; lane 5, 555 bp; lane 6, 681 bp; lane 7, 764 bp; lane 853 bp; and lane 9, 976 bp.

Table I. Relative quantification using the comparative Ct method.

Conservation method	Average Ct	dCt (Ct − (Ct, frozen)	GADPH relative quantity to frozen sample
Frozen	27.37	0.00 ± 0.45	1.0 (0.7–1.4)
Formalin-fixation	33.65	−6.28 ± 0.56	0.012 (0.009–0.019)

The quantity of detectable GAPDH mRNA of frozen samples was defined as 1 while that of formalin-fixed samples was only 0.012.

dCt. As the efficiency of PCR is close to 1 according to Applied Biosystems guidelines, the value of 2^{-dCt} shows the mRNA quantity of PCR level relative to that of the standards. The average relative quantity of the *GAPDH* RT-PCR product is shown in Table I. There was a significant difference between the two groups. Only about 1% of the quantity of PCR product of the frozen samples was obtained using formalin-fixed samples.

Discussion

Analysis of inner ear function has progressed significantly from histological as well as molecular studies on experimental animals. In contrast, pathological study of the inner ear of humans with hearing loss is limited to cases in which brain autopsy is performed because it is impossible to access the inner ear during a patient's lifetime. Furthermore, the inner ear is present in hard bone tissue, and is highly differentiated anatomically and functionally. Therefore, it is difficult to study temporal bone molecular pathology by paraffin-embedded sections, nor can celloidin-embedded sections be relied upon [15].

To analyze real vital reactions at the molecular level, it is necessary to review manifestations of mRNA or protein. RT-PCR, in situ hybridization, Northern blot, or DNA microarrays for mRNA, and Western blot or immunostaining for protein are available for the analysis of vital reactions. However, these methods are usually difficult to apply to human inner ear specimens because these are usually formalin-fixed, celloidin-embedded specimens, which could easily degenerate and cause autolysis of fragile mRNA. Therefore, the human inner ear can be analyzed only for limited purposes. Lee et al. reported the first study of RT-PCR for archival temporal bones in 1997, in which they examined the manifestation of the γ-actin gene [16]. In this report, manifestation of γ-actin was detected in only 1 of 10 archival temporal bone specimens; the authors concluded that examination of the gene expression from an archival section was very limited because mRNA had been degraded by RNases. By contrast, Ohtani et al. reported that the α-tubulin gene was identifiable to 79% by nested RT-PCR in archival temporal bones in 1999 [17]. They concluded that the difference in their study from the former could be explained by the influence of primer design and RNA extraction methods. In formalin-fixed paraffin-embedded archival samples (liver tissue of mice), chemical modification such as methylol addition by formalin does not allow the direct application of extracted RNA to cDNA synthesis and RT-PCR [18].

In the present study, membranous labyrinths were dissected from three formalin-fixed and three frozen temporal bones and RNA was extracted from them. Then we compared the two samples based on how many base pairs of *COCH* mRNA were detectable. In addition, *GAPDH* mRNA was amplified by quantitative RT-PCR, and the quantities of RNA detectable by RT-PCR were compared. As a result, the *COCH* mRNA could be amplified to 976 bp in all the frozen sections, but among the formalin-fixed specimens, two could be amplified only to 249 bp while the other could not be amplified. In addition, the quantity of amplifiable *GAPDH* mRNA in the formalin-fixed specimens was only 1% of that of a frozen section. As a matter of course, both fragment lengths and quantities of RNA of formalin-fixed specimens are overwhelmingly smaller than those of frozen samples. Therefore, formalin-fixed temporal bone samples are not suitable for comprehensive molecular analysis, and conservation by freezing is desirable for introducing molecular pathological tools into human temporal bone pathology.

As for using autopsy specimens, Lin et al. reported RNA analysis of temporal bone soft tissues [10]. They collected temporal bones at immediate autopsies and showed manifestations and localizations of mRNA of mucin genes, such as MUC5B and MUC1, distributed in the submucosal gland of the eustachian tube and the middle ear, by Northern blot technique and in situ hybridization. They described how RNA degrades after death in a time-dependent manner, with the first obvious signs of degradation showing 6 h after death, and found mRNA was up to 1.4 kb in size at 6 h after death, indicating the preferability of an RNA analysis that uses molecular biological techniques within this time-frame.

However, in a regular clinical setting, it is not realistic to perform an autopsy within 6 h of death to obtain a temporal bone, not only from an ethical

perspective but also in terms of cooperation with a pathologist and the difficulty of processing specimens continuously. In our institution, removal of temporal bone specimens is included in the protocol of a conventional autopsy, and the average time from death to autopsy is 10 h. In this time, *COCH* mRNA could be amplified well up to 976 bp, which is the longest fragment expected by our primer planning. A continuous cryopreservation maneuver, which is routinely applied to preserve other organs, enables us to choose appropriate and effective analysis of precious cases. Therefore, our procedure is advantageous in that it can be performed in the protocol of a routine autopsy at any institution. Recently, Robertson et al. constructed a cDNA library from human fetuses at 16–22 weeks developmental age and reported that *COL1A2*, *COL2A2*, and *COL3A1*, which code types I, II, and III collagen, are intensely expressed by comparing expression levels with those of the brain by Northern blot technology [19]. They also reported that *COCH* emerged highly in the inner ear from the cDNA library, and these results led to the identification of *COCH* mutation causing DFNA9 [12,20,21]. Abe et al. extracted RNA from a cochlea obtained in an operation for acoustic neuroma or temporal bone tumor and reported that a strong manifestation of μ-crystallin (*CRYM*) in the membranous labyrinth was shown by the cDNA microarray method [22]. Furthermore, they suggested that *CRYM* mutation causes nonsyndromic deafness by *CRYM*.

In contrast to studies using human fetuses or surgical specimens, we studied autopsy specimens and succeeded in extracting mRNA in comparatively good condition. Using our proposed technique, the human inner ear can be studied by both molecular and histopathologic methods. Therefore, when human temporal bone specimens with almost the same hearing levels on both sides are obtained, we recommend that one side be formalin-fixed and celloidin-embedded and examined morphologically, while the other side be frozen and analyzed for mRNA or other molecules. Comparison of morphological and molecular biological examinations may elucidate pathologies of sensory neural hearing loss at the cellular and molecular level.

Conclusion

Well-preserved mRNA could be extracted from frozen human temporal bones removed at brain autopsy. The present study demonstrates that analysis of mRNA could be a clue in the study of molecular mechanisms of inner ear disorders using human temporal bones.

Acknowledgements

We would like to thank to Mr Kenichi Koizumi for excellent technical support, and Prof. Yukiko Iino and Prof. Yoshihiko Murakami for technical advice. This study was supported by 21st Century COE Program Brain Integration and Its Disorder[s] and a Grant-in-Aid for Scientific Research (nos 14770888, 15790924, 14370539, 17390457, 16659462, 16790 991, 17791163, 16012215, 18791194, 18791193) from the Ministry of Science, Education, Sports and Culture of Japan, and by Health and Labour Sciences Research Grants (H13-006; Research on Sensory and Communicative Disorders, and H14-21, H17-21 and no. 17242101; Research on Measures for Intractable Diseases) from the Ministry of Health, Labour and Welfare of Japan.

References

[1] Gibson F, Walsh J, Mburu P, Varela A, Brown KA, Antonio M, et al. A type VII myosin encoded by the mouse deafness gene shaker-1. Nature 1995;374:62–4.

[2] Everett LA, Belyantseva IA, Noben-Trauth K, Cantos R, Chen A, Thakkar SI, et al. Targeted disruption of mouse Pds provides insight about the inner-ear defects encountered in Pendred syndrome. Hum Mol Genet 2001;10:153–61.

[3] Schuknecht H. Pathology of the ear, 2nd edn. Philadelphia: Lea & Febiger; 1993.

[4] Wackym PA, Simpson TA, Gantz BJ, Smith RJ. Polymerase chain reaction amplification of DNA from archival celloidin-embedded human temporal bone sections. Laryngoscope 1993;103:583–9.

[5] Wacym PA, Popper P, Kerner MM, Grody WW. Varicella-zoster DNA in temporal bones of patients with Ramsay Hunt syndrome. Lancet 1993;342:1555.

[6] Wackym PA. Molecular temporal bone pathology: II. Ramsay Hunt syndrome (Herpes Zoster oticus). Laryngoscope 1997;107:1165–75.

[7] Seidman MD, Bai U, Khan MJ, Murphy MJ, Quirk WS, Castora FL, et al. Association of mitochondrial DNA deletions and cochlear pathology: a molecular biologic tool. Laryngoscope 1996;106:777–83.

[8] Takahashi K, Merchant SN, Miyazawa T, Yamaguchi T, McKenna MJ, Kouda H, et al. Temporal bone histopathological and quantitative analysis of mitochondrial DNA in MELAS. Laryngoscope 2003;113:1362–8.

[9] Kimura Y, Kouda H, Kobayashi D, Suzuki Y, Ishige I, Iino Y, et al. Detection of mitochondrial DNA from human inner ear using real-time polymerase chain reaction and laser microdissection. Acta Otolaryngol (Stockh) 2005;125:697–701.

[10] Lin J, Kawano H, Paparella MM, Ho SB. Improved RNA analysis for immediate autopsy of temporal bone soft tissues. Acta Otolaryngol (Stockh) 1999;119:787–95.

[11] Smith CA, Vernon JA. Handbook of auditory and vestibular research methods. Springfield, IL: Charles C Thomas; 1976. p. 5–51.

[12] Robertson NG, Skvorak AB, Yin Y, Weremowicz S, Johnson KR, Kovatch KA, et al. Mapping and characterization of a novel cochlear gene in human and in mouse: a positional candidate gene for a deafness disorder, DFNA9. Genomics 1997;15:345–54.

[13] Lehmann U, Glöckner S, Kleeberger W, von Wasielewski HF, Kreipe H. Detection of gene amplification in archival breast cancer specimens by laser assisted microdissection and quantitative real-time polymerase chain reaction. Am J Pathol 2000;156:1855–64.

[14] Bloch G, Toma DP, Robinson GE. Behavioral rhythmicity, age, division of labor and period expression in the honey bee brain. J Biol Rhythms 2001;16:444–56.

[15] Merchant SN, Burgess B, O'Malley J, Jones D, Adams JC. Polyester wax: a new embedding medium for the histopathologic study of human temporal bones. Laryngoscope 2006; 116:245–9.

[16] Lee KH, McKenna MJ, Sewell WF, Ung F. Ribonucleases may limit recovery of ribonucleic acids from archival human temporal bones. Laryngoscope 1997;107:1228–34.

[17] Ohtani F, Furuta Y, Iino Y, Inuyama Y, Fukuda S. Amplification of RNA from archival human temporal bone sections. Laryngoscope 1999;109:617–20.

[18] Masuda N, Ohnishi T, Kawamoto S, Monden M, Okubo K. Analysis of chemical modification of RNA from formalin-fixed samples and optimization of molecular biology applications for such samples. Nucleic Acids Res 1999;27:4436–43.

[19] Robertson NG, Khetarpal U, Gutierrez-Espeleta GA, Bieber FR, Morton CC. Isolation of novel and known genes from a human fetal cochlear cDNA library using subtractive hybridization and differential screening. Genomics 1994;23: 42–50.

[20] Robertson NG, Lu L, Heller S, Merchant SN, Eavey RD, McKenna M, et al. Mutations in a novel cochlear gene cause DFNA9, a human nonsyndromic deafness with vestibular dysfunction. Nat Genet 1998;20:299–303.

[21] Robertson NG, Cremers CW, Huygen PL, Ikezono T, Krastins B, Kremer H, et al. Cochlin immunostaining of inner ear pathologic deposits and proteomic analysis in DFNA9 deafness and vestibular dysfunction. Hum Mol Genet 2006;15:1071–85.

[22] Abe S, Katagiri T, Saito-Hisaminato A, Usami S, Inoue Y, Tsunoda T, et al. Identification of CRYM as a candidate responsible for nonsyndromic deafness, through cDNA microarray analysis of human cochlear and vestibular tissues. Am J Hum Genet 2003;72:73–82.